Status of the Virgo project

T Accadia, F Acernese, F Antonucci, P Astone, G Ballardin, F Barone, M Barsuglia, A Basti, Th S Bauer, M Bebronne, et al.

Status of the Virgo project

T. Accadia[1], **F. Acernese**[2ac], **F. Antonucci**[3a], **P. Astone**[3a], **G. Ballardin**[4], **F. Barone**[2ac], **M. Barsuglia**[5], **A. Basti**[6ab], **Th. S. Bauer**[7a], **M. Bebronne**[1], **M.G. Beker**[7a], **A. Belletoile**[1], **S. Birindelli**[8a], **M. Bitossi**[6a], **M. A. Bizouard**[9a], **M. Blom**[7a], **F. Bondu**[8b], **L. Bonelli**[6ab], **R. Bonnand**[10], **V. Boschi**[6a], **L. Bosi**[11a], **B. Bouhou**[5], **S. Braccini**[6a], **C. Bradaschia**[6a], **M. Branchesi**[12ab], **T. Briant**[13], **A. Brillet**[8a], **V. Brisson**[9a], **R. Budzyński**[14b], **T. Bulik**[14bc], **H. J. Bulten**[7ab], **D. Buskulic**[1], **C. Buy**[5], **G. Cagnoli**[12a], **E. Calloni**[2ab], **B. Canuel**[4], **F. Carbognani**[4], **F. Cavalier**[9a], **R. Cavalieri**[4], **G. Cella**[6a], **E. Cesarini**[12b], **O. Chaibi**[8a], **E. Chassande-Mottin**[5], **A. Chincarini**[15], **F. Cleva**[8a], **E. Coccia**[16ab], **P.-F. Cohadon**[13], **C. N. Colacino**[6ab], **J. Colas**[4], **A. Colla**[3ab], **M. Colombini**[3b], **A. Corsi**[3a], **J.-P. Coulon**[8a], **E. Cuoco**[4], **S. D'Antonio**[16a], **V. Dattilo**[4], **M. Davier**[9a], **R. Day**[4], **R. De Rosa**[2ab], **G. Debreczeni**[17], **W. Del Pozzo**[7a], **M. del Prete**[18b], **L. Di Fiore**[2a], **A. Di Lieto**[6ab], **M. Di Paolo Emilio**[16ac], **A. Di Virgilio**[6a], **A. Dietz**[1], **M. Drago**[18ab], **V. Fafone**[16ab], **I. Ferrante**[6ab], **F. Fidecaro**[6ab], **I. Fiori**[4], **R. Flaminio**[10], **L. A. Forte**[2a], **J.-D. Fournier**[8a], **J. Franc**[10], **S. Frasca**[3ab], **F. Frasconi**[6a], **M. Galimberti**[10], **L. Gammaitoni**[11ab], **F. Garufi**[2ab], **M. E. Gáspár**[17], **G. Gemme**[15], **E. Genin**[4], **A. Gennai**[6a], **A. Giazotto**[6a], **R. Gouaty**[1], **M. Granata**[5], **C. Greverie**[8a], **G. M. Guidi**[12ab], **J.-F. Hayau**[8b], **A. Heidmann**[13], **H. Heitmann**[8], **P. Hello**[9a], **D. Huet**[4], **P. Jaranowski**[14d], **I. Kowalska**[14b], **A. Królak**[14ae], **N. Leroy**[9a], **N. Letendre**[1], **T. G. F. Li**[7a], **N. Liguori**[18ab], **M. Lorenzini**[12a], **V. Loriette**[9b], **G. Losurdo**[12a], **E. Majorana**[3a], **I. Maksimovic**[9b], **N. Man**[8a], **M. Mantovani**[6ac], **F. Marchesoni**[11a], **F. Marion**[1], **J. Marque**[4], **F. Martelli**[12ab], **A. Masserot**[1], **C. Michel**[10], **L. Milano**[2ab], **Y. Minenkov**[16a], **M. Mohan**[4], **N. Morgado**[10], **A. Morgia**[16ab], **S. Mosca**[2ab], **V. Moscatelli**[3a], **B. Mours**[1], **F. Nocera**[4], **G. Pagliaroli**[16ac], **L. Palladino**[16ac], **C. Palomba**[3a], **F. Paoletti**[6a,4], **M. Parisi**[2ab], **A. Pasqualetti**[4], **R. Passaquieti**[6ab], **D. Passuello**[6a], **G. Persichetti**[2ab], **M. Pichot**[8a], **F. Piergiovanni**[12ab], **M. Pietka**[14d], **L. Pinard**[10], **R. Poggiani**[6ab], **M. Prato**[15], **G. A. Prodi**[18ab], **M. Punturo**[11a], **P. Puppo**[3a], **D. S. Rabeling**[7ab], **I. Rácz**[17], **P. Rapagnani**[3ab], **V. Re**[16ab], **T. Regimbau**[8a], **F. Ricci**[3ab], **F. Robinet**[9a], **A. Rocchi**[16a], **L. Rolland**[1], **R. Romano**[2ac], **D. Rosińska**[14cf], **P. Ruggi**[4],

B. Sassolas[10], D. Sentenac[4], L. Sperandio[16ab], R. Sturani[12ab], B. Swinkels[4], M. Tacca[4], L. Taffarello[18c], A. Toncelli[6ab], M. Tonelli[6ab], O. Torre[6ac], E. Tournefier[1], F. Travasso[11ab], G. Vajente[6ab], J. F. J. van den Brand[7ab], C. Van Den Broeck[7a], S. van der Putten[7a], M. Vasuth[17], M. Vavoulidis[9a], G. Vedovato[18c], D. Verkindt[1], F. Vetrano[12ab], A. Viceré[12ab], J.-Y. Vinet[8a], S. Vitale[7a], H. Vocca[11a], R. L. Ward[5], M. Was[9a], M. Yvert[1], J.-P. Zendri[18c]

[1]Laboratoire d'Annecy-le-Vieux de Physique des Particules (LAPP), Université de Savoie, CNRS/IN2P3, F-74941 Annecy-Le-Vieux, France
[2]INFN, Sezione di Napoli [a]; Università di Napoli 'Federico II'[b] Complesso Universitario di Monte S.Angelo, I-80126 Napoli; Università di Salerno, Fisciano, I-84084 Salerno[c], Italy
[3]INFN, Sezione di Roma[a]; Università 'La Sapienza'[b], I-00185 Roma, Italy
[4]European Gravitational Observatory (EGO), I-56021 Cascina (PI), Italy
[5]Laboratoire AstroParticule et Cosmologie (APC) Université Paris Diderot, CNRS: IN2P3, CEA: DSM/IRFU, Observatoire de Paris, 10 rue A.Domon et L.Duquet, 75013 Paris - France
[6]INFN, Sezione di Pisa[a]; Università di Pisa[b]; I-56127 Pisa; Università di Siena, I-53100 Siena[c], Italy
[7]Nikhef, Science Park, Amsterdam, the Netherlands[a]; VU University Amsterdam, De Boelelaan 1081, 1081 HV Amsterdam, the Netherlands[b]
[8]Université Nice-Sophia-Antipolis, CNRS, Observatoire de la Côte d'Azur, F-06304 Nice[a]; Institut de Physique de Rennes, CNRS, Université de Rennes 1, 35042 Rennes[b], France
[9]LAL, Université Paris-Sud, IN2P3/CNRS, F-91898 Orsay[a]; ESPCI, CNRS, F-75005 Paris[b], France
[10]Laboratoire des Matériaux Avancés (LMA), IN2P3/CNRS, F-69622 Villeurbanne, Lyon, France
[11]INFN, Sezione di Perugia[a]; Università di Perugia[b], I-06123 Perugia,Italy
[12]INFN, Sezione di Firenze, I-50019 Sesto Fiorentino[a]; Università degli Studi di Urbino 'Carlo Bo', I-61029 Urbino[b], Italy
[13]Laboratoire Kastler Brossel, ENS, CNRS, UPMC, Université Pierre et Marie Curie, 4 Place Jussieu, F-75005 Paris, France
[14]IM-PAN 00-956 Warsaw[a]; Astronomical Observatory Warsaw University 00-478 Warsaw[b]; CAMK-PAN 00-716 Warsaw[c]; Białystok University 15-424 Białystok[d]; IPJ 05-400 Świerk-Otwock[e]; Institute of Astronomy 65-265 Zielona Góra[f], Poland
[15]INFN, Sezione di Genova; I-16146 Genova, Italy
[16]INFN, Sezione di Roma Tor Vergata[a]; Università di Roma Tor Vergata, I-00133 Roma[b]; Università dell'Aquila, I-67100 L'Aquila[c], Italy
[17]RMKI, H-1121 Budapest, Konkoly Thege Miklós út 29-33, Hungary
[18]INFN, Gruppo Collegato di Trento[a] and Università di Trento[b], I-38050 Povo, Trento, Italy; INFN, Sezione di Padova[c] and Università di Padova[d], I-35131 Padova, Italy

E-mail: krolak@impan.gov.pl

Abstract. We describe the present state and future evolution of the Virgo gravitational wave detector, realized by the Virgo Collaboration at the European Gravitational Observatory, in Cascina near Pisa in Italy. We summarize basic principles of the operation and the design features of the Virgo detector. We present the sensitivity evolution due to a series of intermediate upgrades called Virgo+ which is being completed this year and includes new monolithic suspensions. We describe the present scientific potential of the detector. Finally we discuss the plans for the second generation of the detector, called Advanced Virgo, introducing its new features, the expected sensitivity evolution and the scientific potential.

PACS numbers: 04.80.Nn, 95.55.Ym

Figure 1. An aerial view of the Virgo gravitational wave detector. The detector Virgo is located in the countryside of Commune of Cascina, a few km south of the city of Pisa, Tuscany.

1. Introduction

The first generation of km-scale interferometric gravitational-wave detectors Virgo [1], LIGO [2] and GEO600 [3] are engaged in a search for gravitational-waves from astronomical sources. These projects form an international collaboration that analyzes jointly the data from all the detectors. Gravitational waves have not been detected yet, but searches for sources like binary systems of neutron stars and/or black holes, energetic bursts, rotating isolated neutron stars and a gravitational wave background from the early universe have led to upper limits (see Section 6 for more details). These upper limits are beginning to provide an important astrophysical information about the Universe and thereby opening a new observational field - the gravitational wave astronomy. In this paper we shall review the current status of one of the gravitational-wave detectors - the Virgo project.

2. Virgo project

Virgo is the gravitational wave detector funded by CNRS (France) and INFN (Italy). Its construction was completed in June 2006. Virgo is a recycled Michelson interferometer with 3 km-long Fabry-Perot cavities in its arms. Virgo is located at the European Gravitational Observatory (EGO), close to Cascina (Pisa, Italy). It is the only ground-based antenna that, from its conception, aimed at reducing the detection band lower threshold down to 10 Hz. This goal has been achieved by isolating the interferometer mirrors from seismic noise which, in the tens of Hz range, is many orders of magnitude larger than the small variation of the arm length induced by the gravitational wave passage. In recent years other European research groups (from Holland, Poland, Hungary, and UK) have joined the collaboration. An aerial view of the Virgo detector is shown in Figure 1.

3. Virgo detector

In Figure 2 we present diagram of the optical design of the Virgo detector. The laser beam, after passing through the optical table for its alignment, enters the vacuum system, reaching the input optical bench (IB). The beam is then spatially filtered by a 144 m-long triangular cavity (input mode cleaner - IMC). This additional cavity selects the optical fundamental mode (the Gaussian TEM00 mode), suppressing the high-order modes. The IMC is also used as a reference to pre-stabilize the laser beam frequency. The IMC length is stabilized in the low frequency range (below a few tens of Hz, where seismic noise and other spurious mechanisms induce fluctuations of the cavity length) by using as a reference a rigid 30 cm-long reference cavity (RFC). After the IMC, the beam passes through the power recycling mirror (PR), is separated by the beam splitter (BS) and enters the two 3km long Fabry-Perot cavities. The power recycling mirror forms an additional Fabry-Perot cavity between the whole interferometer and itself. In this way the power impinging onto the BS is amplified by a factor of 50. The output interference signal is reconstructed by the photodiode B1, made by a set of high-quantum efficiency photodiodes. The output beam, before reaching B1, passes through a monolithic 2.5 cm-long cavity (output mode cleaner - OMC). The OMC is designed to filter high-order optical modes, originating from misalignments and optical defects. The other photodiodes (labeled by B in Fig.2) are used as feedback error signals to fix the longitudinal lengths of the interferometer (cavity resonance condition and destructive interference on B1) with a very high level of accuracy. In order to optimize the contrast in the interference pattern, the interferometer mirrors must be aligned with each another and with respect to the beam with a nanoradian accuracy. This is done using a feedback based on the error signals coming from the quadrant photodiodes (labeled by Q in Fig.2). All the six main Virgo mirrors: Power Recycling, Beam Splitter, North Input, North End, West Input, West End (see Fig.2 with obvious notations) are suspended from a superattenuator (see Fig.3). In order to reduce the variations of the refraction index due to the gas density fluctuations the entire interferometer must be kept in the vacuum. For this reason, each of the long Fabry-Perot cavities is contained in a 3 km-long vacuum pipe, with a diameter of 1.2 m. The seismic isolation is provided by passive five pendulum system called the superattenuator (see Fig.3 the plot on the left) what allows a very large suppression of the thermal noise by more than 10 orders of magnitude starting from a few Hz (see Fig.3 the plot on the right).

4. Virgo upgrades

The commissioning of the Virgo detector lasted from the year 2003 to 2007. In 2007 from 18th of May till 1st of October the first Virgo scientific run (VSR1) took place (136 days) (see [4, 5]). At the end of VSR1, in October 2007, an intense program of upgrades and commissioning started to lead the detector towards the Virgo+ configuration. The main upgrades regarded the installation of a better and less noisy read-out and control electronics, the installation of a more powerful laser amplifier and some upgrades of the injection bench necessary to cope with the higher laser power and to provide a better seismic noise rejection. Moreover, a thermal compensation system (TCS) [9] has been installed to reduce thermal effects in the input mirrors. TCS uses a CO_2 beam that heats the peripheral of the input test masses in order to compensate for the deformation induced in the mirror central area by the heat deposited by the main

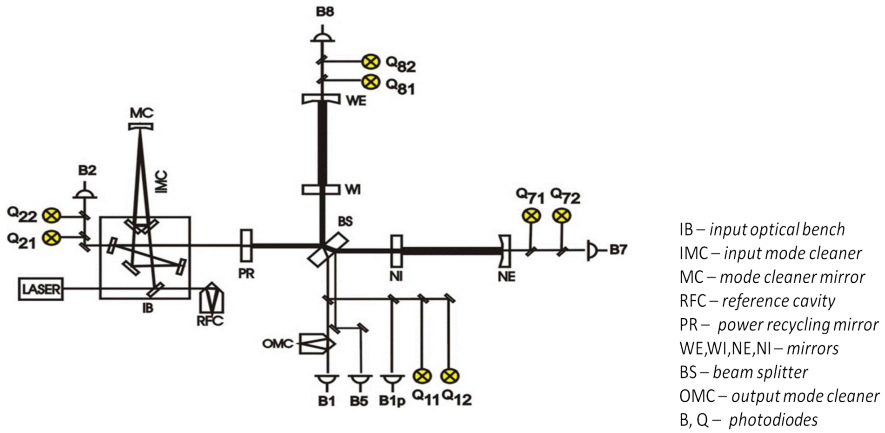

Figure 2. The optical layout of the Virgo detector.

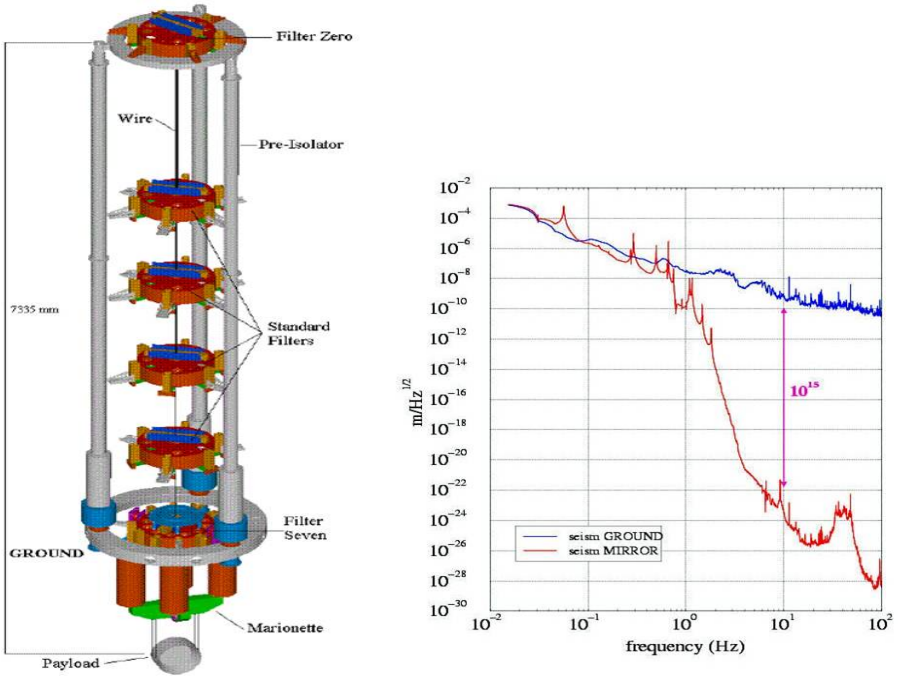

Figure 3. The left panel is the image of the entire Virgo superattenuator. The right panel presents comparison of the spectral density of seismic noise at the ground and that at the mirror. The Virgo superattenuator provides suppression of the amplitude spectral density of noise by 15 orders of magnitude at 10 Hz frequency.

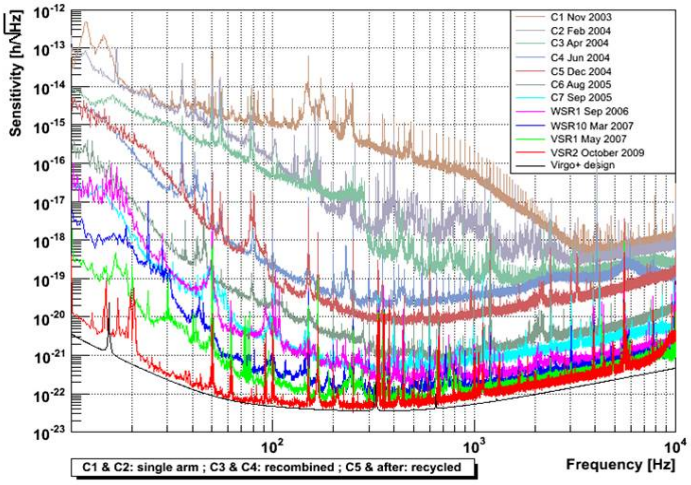

Figure 4. Amplitude spectral density of noise of the Virgo detector during various stages of commissioning and during the science runs VSR1 and VSR2 in comparison to Virgo+ design sensitivity curve.

mirror. The commissioning activity allowed to increase the input power from 8 W, used during VSR1, to 17 W. After these upgrades Virgo performed the second science run (VSR2) that lasted from 7th of June 2009 till 7th of January 2010 (183 days) (see [6]). In Figure 4 we compile sensitivities of the Virgo detector during various stages of commissioning and the science run. We note that the measured Virgo sensitivity towards the end of VSR2 was very close to the design curve. After the end of VSR2 run Virgo has started the installation of monolithic suspensions leading to Virgo+MS configuration (see [7, 8]). This should allow a reduction of thermal noise level in the frequency region around 30-40 Hz. If combined with an increase of the cavity finesse and with the replacement of the test masses with new mirrors exhibiting a lower thermal noise level, it is possible to extend several times the horizon distance for the detection of compact coalescing binaries. In order to have a fully monolithic stage, fused silica wires have to be properly attached to the mirror. This is possible by means of suitable silica supports (called *ears*) bonded to the mirror sides through the silicate bonding technique [10, 11, 12]. Moreover, they have to be clamped in a proper way to the upper stage of suspension, minimizing the impact on the overall suspension design (see Figure 5). The installation of monolithic suspensions was successful but unfortunately it turned out that the radius of curvature (ROC) of the NE end mirror was shorter that that of the WE mirror by 110m. This led to more total light at the output port (greater contrast defect) and thus more scattered light in the detection bench. As a result the power of the light at the dark fringe was around 3 watts (ten times larger than in Virgo). The main contribution of the noise has come from the beam reflected by the output mode cleaner. Consequently this beam was dumped outside the vacuum. However the scattering noises still occurred originating probably at the output window and on the dumper itself. Despite these problems in order to take data in coincidence with the LIGO detectors Virgo has started the third science

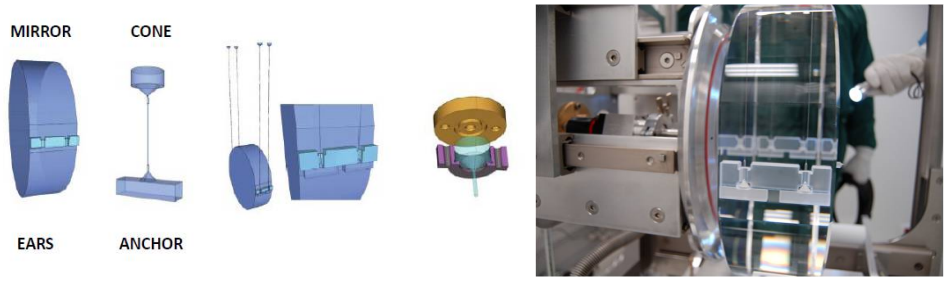

Figure 5. Monolitic suspension. The images, looking from the left, are respectively: the mirror with two ears silicate bonded to its side, silica wire with the upper end welded to the silica cone and the lower ended welded to the silica anchor, mirror suspended by four wires using anchors, close up of the anchor attachment, close up of the cone suspension, and the suspended mirror in position at the Virgo site.

run (VSR3). After the closing of VSR3, the first action will be to dump under vacuum the beam most critical for the resulting scattered light. Then a first short campaign of measurements in the 150-300 Hz region will be done. After that it is expected to install the system for the radius of curvature compensation. It has been decided to increase the radius of curvature of the NE mirror to match that of WE mirror by frontal heating. These actions should result in an improved sensitivity and another data run - VSR4 is planned in the mid 2011, to be followed by the start of the Advanced Virgo installation. It is still not possible to predict what the sensitivity of the Virgo detector will be during the VSR4 data run.

5. Advanced Virgo

The Advanced Virgo funding has been approved by INFN and CNRS at the end of 2009. In order to increase the interferometer sensitivity at higher frequencies the laser input power will be around 200 W (with 125 W injected into the interferometer). The baseline design [13] foresees the use of a solid state laser composed by a stabilized master laser followed by two stages of amplification. To cope with the larger radiation pressure effects due to the larger power injected the heavier test masses (42 kg) will be used, and as in the Virgo+MS, they will be suspended through the fused silica fibers. The installation of heavier monolithic suspension mirrors will further increase sensitivity below 50Hz with respect to the Virgo+MS configuration. To this extent, the experience done with the Virgo+MS payloads will be precious to understand all the features of this technology, improve it further and reduce the risk for the advanced detectors. The optical scheme is modified by the introduction of a signal recycling cavity. The use of signal recycling [14] and of the resonant sideband extraction scheme allows widening the detector bandwidth thus extending the sensitivity into the kHz region. By changing the position of the signal recycling mirror one can optimize the sensitivity of the detector for various gravitational wave sources. Also the finesse of the 3 km Fabry-Perot cavities will be larger (around 900 in the baseline). A DC detection scheme will be adopted to reduce some technical noises instead of the RF scheme used in the initial Virgo. The vacuum system and the infrastructures will be also upgraded to improve the sensitivity in the low and mid frequency range. Large cryotraps will

be installed at the extremes of the 3 km vacuum pipes to isolate them from the rest of the vacuum system. This, combined with the baking of the tubes, will allow reducing the residual gas pressure to the target of 10^{-9} mbar. To reduce the risk of acoustic couplings, the air conditioning machines as well as several other sources of acoustic noise will be moved out of the central experimental hall. The reference sensitivity for Advanced Virgo in comparison with design Virgo+ and Virgo+MS sensitivities is shown in Figure 6. Around 100 Hz the main limitation to the sensitivity is due to the

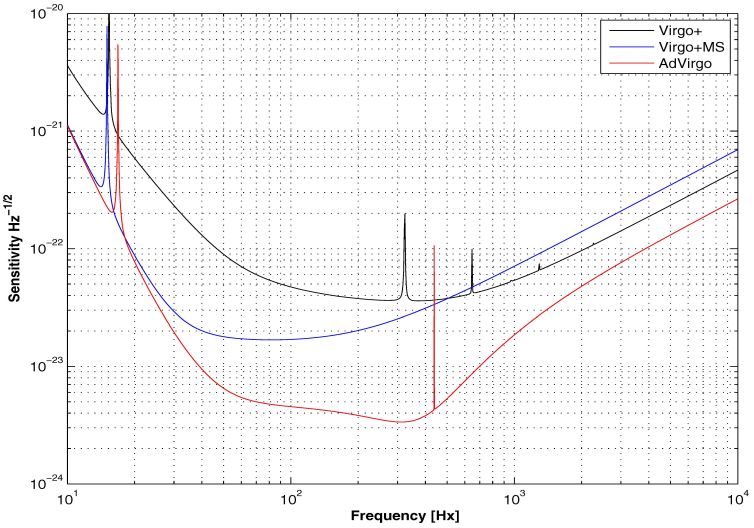

Figure 6. Design sensitivities of the Virgo detector.

thermal noise in the mirror coatings. The sensitivity shown in the Figure 6 assumes current coating technology. Any further improvements from the ongoing R&D will have a direct positive impact on the detector sensitivity. The effect of coating thermal noise is minimized running the Fabry-Perot cavities near the co-focal configuration thus maximizing the beam size on the mirrors.

According to the present planning Virgo+ will be shut down in the second half of 2011 and the installation of Advanced Virgo will start. The commissioning of the interferometer should start in 2014 with the goal of having a first stable 1-hour lock in 2015.

6. Virgo performance

The most promising source of gravitational waves that can be detected with ground based laser interferometers is the coalescence of compact binaries consisting of neutron stars and/or black holes. Thanks to intensive research of relativists, astrophysicists and computer scientists we can predict the gravitational wave signal from a coalescing binary extremely well [15, 16]. This signal sweeps through the detector frequency band and the range to which a signal could be detected provides a very good overall characteristic of the performance of the detector. The basic quantity is the *horizon distance* which is the distance to an optimally oriented binary source that can be detected with signal-to-noise ratio (SNR) equal to 8 (see [17] Sec. III). A commonly

Table 1. Expected horizons and detection rates of coalescing binaries during the two Virgo science runs. Actual sensitivities reached will depend on the real performance of the detectors.

Run	NS-NS	NS-BH	BH-BH
VSR1			
H [Mpc]	4.0	7.9	18
R [no./yr]	3.1×10^{-4}	7.1×10^{-5}	1.0×10^{-4}
VSR2			
H [Mpc]	9.8	20	46
R [no./yr]	4.5×10^{-3}	1.2×10^{-3}	1.9×10^{-3}

used characteristic is the *sensemon range* defined as the radius of a sphere whose volume is equal to the volume in which an interferometer could detect a source at SNR = 8, taking all possible sky locations and orientations into account. The sensemon range is smaller than the horizon distance by factor of around 2.26. In Figure 7 we have shown evolution of the sensemon range during the Virgo data taking VSR1 and VSR2. An uncertain factor about the detection of coalescing compact binaries is the rate

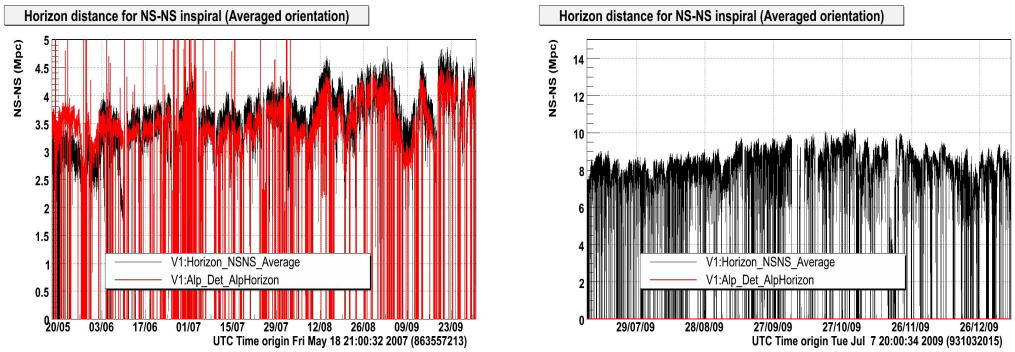

Figure 7. Sensemon range during VSR1 (left panel) and VSR2 (right panel). On the left panel two independent estimations of the sensemon range are displayed.

of occurrence of these sources (see [17] for a comprehensive discussion of the current understanding of the population of these sources in our Universe). In Tables 1 and 2 we have presented sensemon ranges H in Mpc and estimated detection rates R in number of sources per year during the three Virgo science runs and for three design sensitivities of Virgo detector. We have used so-called realistic rates of compact binary coalescences summarized in Table IV of [17]. We see that with VSR1 and VSR2 data detection of a coalescing binary gravitational wave signal is very unlikely however it should be very common with the Advanced Virgo detector. The Virgo data, together with the LIGO and GEO600 data, are searched for gravitational wave signals from all types of astrophysical sources: coalescing binaries, supernovae, rotating neutron stars, early Universe. So far there were no detections but a number of astrophysically significant limits is being imposed [18, 19, 20, 21, 22, 23]. This is consistent with the present sensitivity of the Virgo detector and the current astrophysical understanding of the gravitational wave generation mechanisms. For example with a very good sensitivity of the Virgo detector at low frequencies the spin down limit for the Vela pulsar

Table 2. Expected detection rates of coalescing binaries for Virgo design sensitivities.

Design	NS-NS	NS-BH	BH-BH
Virgo+			
H [Mpc]	14	28	65
R [no./yr]	1.3×10^{-2}	3.3×10^{-3}	5.2×10^{-3}
Virgo+MS			
H [Mpc]	50	110	250
R [no./yr]	6.1×10^{-1}	1.7×10^{-1}	3.2×10^{-1}
AdVirgo			
H [Mpc]	150	320	730
R [no./yr]	17	4.7	7.6

will certainly be beaten. Virgo together with LIGO detectors is also receiving and providing triggers from coincident searches with other astronomical projects: gamma ray burst detectors [19, 21], wide-field optical telescopes and high energy neutrinos detectors. In particular Virgo detector is indispensable in obtaining position in the sky of the triggers because this requires data from at least three detectors.

6.1. Acknowledgments

The authors acknowledge the support of the Italian Istituto Nazionale di Fisica Nucleare and the French Centre National de la Recherche Scientifique for the construction and operation of the Virgo detector. The authors also gratefully acknowledge the support of the research by these agencies and by the Foundation for Fundamental Research on Matter supported by the Netherlands Organization for Scientific Research, the Polish Ministry of Science and Higher Education, the FOCUS Programme of Foundation for Polish Science.

References

[1] http://wwwcascina.virgo.infn.it/
[2] http://www.ligo.caltech.edu/
[3] http://www.geo600.uni-hannover.de/
[4] Acernese F et al. (Virgo Collaboration), 2008, Class. Quantum Grav. 25(11) 114045
[5] Acernese F et al. (Virgo Collaboration), 2008, Class. Quantum Grav. 25(9) 184001
[6] Accadia T et al. (Virgo Collaboration), 2010, J. Phys.: Conf. Ser. 20, 3 012074
[7] Amico P et al., 2001, Rev. Sci. Instrum. 73(9) 3318
[8] Lorenzini M (on behalf of Virgo Collaboration), 2010, Class. Quantum Grav. 27(8) 084021
[9] Accadia et al. *A Thermal Compensation System for the gravitational wave detector Virgo*, in Proceedings of the Twelfth Marcel Grossmann Meeting on General Relativity, edited by Thibault Damour, Robert T Jantzen and Remo Ruffini, World Scientific, Singapore, 2011
[10] Gwo D H *Ultra precision and reliable bonding method*, United States Patent no US 6284085 B1 (2001)
[11] Gretarsson A M et al., 2000, Physics Letters A 270 108
[12] Smith J R et al., 2004, Class. Quantum Grav. 21 S1091
[13] The Virgo Collaboration *Advanced Virgo Baseline Design* available at http://wwwcascina.virgo.infn.it/advirgo/docs.html (2009)
[14] Meers B J, 1988, Phys. Rev. D38 2317
[15] Blanchet L, 2002, Living Rev. Rel. 5 3
[16] Buonanno A, 2007, Phys. Rev. D75 124018
[17] Abadie J et al., 2010, Class. Quant. Grav. 27 173001
[18] The LIGO Scientific Collaboration & The Virgo Collaboration, 2009, Nature 460 990

[19] Abadie J et al., 2010, Astrophys. J 715 1438
[20] Abadie J et al., 2010, Astrophys. J 713 671
[21] Abadie J et al., 2010, Astrophys. J 715 1453
[22] Abadie J et al., 2010, Phys. Rev. D81 102001
[23] Abadie J et al., 2010, Phys. Rev. D82 102001